THE JOURNAL OF BIOLOGICAL CHEMISTRY VOL. 281, NO. 18, pp. 12968–12975, May 5, 2006

Complementation of One RecA Protein Point Mutation by Another

EVIDENCE FOR TRANS CATALYSIS OF ATP HYDROLYSIS[*]

Received for publication, December 27, 2005, and in revised form, March 7, 2006 Published, JBC Papers in Press, March 8, 2006, DOI 10.1074/jbc.M513736200

Julia M. Cox, Stephen N. Abbott, Sindhu Chitteni-Pattu, Ross B. Inman, and Michael M. Cox[1]

From the Department of Biochemistry, University of Wisconsin, Madison, Wisconsin 53706-1544

The RecA residues Lys^{248} and Glu^{96} are closely opposed across the RecA subunit-subunit interface in some recent models of the RecA nucleoprotein filament. The K248R and E96D single mutant proteins of the *Escherichia coli* RecA protein each bind to DNA and form nucleoprotein filaments but do not hydrolyze ATP or dATP. A mixture of K248R and E96D single mutant proteins restores dATP hydrolysis to 25% of the wild type rate, with maximum restoration seen when the proteins are present in a 1:1 ratio. The K248R/E96D double mutant RecA protein also hydrolyzes ATP and dATP at rates up to 10-fold higher than either single mutant, although at a reduced rate compared with the wild type protein. Thus, the K248R mutation partially complements the inactive E96D mutation and vice versa. The complementation is not sufficient to allow DNA strand exchange. The K248R and E96D mutations originate from opposite sides of the subunit-subunit interface. The functional complementation suggests that Lys^{248} plays a significant role in ATP hydrolysis in *trans* across the subunit-subunit interface in the RecA nucleoprotein filament. This could be part of a mechanism for the long range coordination of hydrolytic cycles between subunits within the RecA filament.

Homologous DNA recombination is a vital component of DNA metabolism, central to processes such as recombinational DNA repair of stalled replication forks and the exchange of genetic material during meiosis in eukaryotes and conjugation in prokaryotes. RecA protein is the central recombinase in *Escherichia coli*, and RecA homologues are present in nearly every organism. In *E. coli*, RecA participates not only in the restart of stalled replication forks but also the induction of the SOS response upon cellular DNA damage distress and translesion DNA synthesis via the error-prone DNA polymerase V (1–3).

RecA protein functions as a nucleoprotein filament. When bound to DNA, RecA promotes the hydrolysis of ATP or dATP. Hydrolysis occurs uniformly throughout the filament. ATP hydrolysis is important for some RecA processes including net disassembly of the nucleoprotein filament, bypass of heterologous insertions during DNA three-strand exchange, complete DNA strand exchange with DNA substrates longer than ~3 kbp, and strand exchange with four DNA strands (1, 4–8). The ATP hydrolytic cycles between adjacent subunits in the RecA filament bound to double-stranded DNA (dsDNA)[2] are coordinated such that waves of hydrolysis move sequentially through the filament with a separation of six subunits (9). RecA could potentially use the organized waves of ATP hydrolysis to act as a motor, driving completion of strand exchange beyond the barriers mentioned above, or to promote replication fork regression (10, 11). The detailed mechanism by which the ATP hydrolysis is coordinated in the RecA-dsDNA nucleoprotein filament is currently unknown.

RecA is a member of an ATPase family with characteristic single or multiple RecA-like folds, composed of a central β-sheet flanked by α-helices. The ATPase family includes helicases like PcrA, ABC transporters, and with relatively less structural similarity, the AAA+ family of ATPases including ClpA (12). These proteins all use the energy from ATP hydrolysis to move macromolecules or move along macromolecules, and hence, may be considered molecular motors. A sequence alignment of RecA and helicases including DnaB (13) highlights the similarities. The authors call attention to a new motif, the [KR]×[KR] motif. This motif is conserved among the DnaB, RecA, Sms, and KaiC families, although absent from the archaean or eukaryotic homologues of RecA.

The [KR]×[KR] motif is involved in the in *trans* catalysis of ATP hydrolysis for some RecA homologues including gp4 of bacteriophage T7 (13–16). The helicase domain of T7 gp4 constitutes a 5′ to 3′ hexameric ring helicase. The crystal structure of a gp4 fragment that retains hexamer formation and helicase activities (residues 241–566) (15) strays from 6-fold rotational symmetry. Indeed, only four of six subunits have bound nucleotide (ADPNP). Arg^{522} is the third residue in the [KR]×[KR] motif, and in the four subunits that bind ADPNP, Arg^{522} is close (~3.5 Å) to the γ-phosphate of the bound nucleotide of the neighboring subunit. However, Arg^{522} is displaced in the two nucleotide-free subunits to more than 10 Å away from the equivalent position where the nucleotide would be bound. A conformational change such as this is suggested to couple hydrolysis and helicase activity. It is proposed that Arg^{522} of T7 gp4 senses hydrolysis of ATP, communicates the hydrolysis between subunits, and promotes conformational changes associated with ATP hydrolysis (14–16). In this manner, Arg^{522} would mimic an arginine finger, as is found in Ras and its GTPase-activating protein (GAP). In the Ras-GAP system, it is postulated that Arg^{789} of GAP similarly reaches across the GAP-Ras interface to stabilize the γ-phosphate of the Ras-bound ATP (17).

Another example of in *trans* catalysis is the RuvB protein (18–20). The RuvB protein is an ATPase that forms a hexameric ring and complexes with RuvA to promote branch migration that is dependent on ATP hydrolysis. Although this protein exhibits some structural similarity to RecA, it appears to lack the [KR]×[KR] motif. The crystal structure features a dimer of *Thermus thermophilus* RuvB, with each subunit having three domains (labeled N, M, and C). The nucleotide is bound between the N and M domains (19). The structure of each subunit is very similar, except for the area immediately around the bound nucle-

* This work was supported by Grant GM52725 from the National Institutes of Health. The costs of publication of this article were defrayed in part by the payment of page charges. This article must therefore be hereby marked "*advertisement*" in accordance with 18 U.S.C. Section 1734 solely to indicate this fact.

[1] To whom correspondence should be addressed: Dept. of Biochemistry, University of Wisconsin, 433 Babcock Dr., Madison, WI 53706-1544. Tel.: 608-262-1181; Fax. 608-265-2603; E-mail: cox@biochem.wisc.edu.

[2] The abbreviations used are: dsDNA, double-stranded DNA; ATPγS, adenosine 5′-*O*-(3-thiotriphosphate); PEP, phosphoenolpyruvate; SSB, single-stranded DNA-binding protein of *Escherichia coli*; ssDNA, single-stranded DNA; GAP, GTPase-activating protein; ADPNP, 5′-adenylyl-β,γ-imidodiphosphate.

otide. One subunit appears to have a triphosphate bound, while the other appears to lack a γ-phosphate; the authors postulated that the structural differences between the subunits could reflect conformational changes dependent on ATP hydrolysis. The crystal structures of wild type and several point mutants of *Thermatoga maritima* RuvB also indicate ADP is bound between two domains of the RuvB subunit (18), suggesting to the authors that the state of the bound nucleotide guides conformational changes between RuvB subunits. More specifically, sensor 1, Walker A, and Walker B were proposed to sense the γ-phosphate and divalent cation, while sensor 2 would accommodate the sugar ring and diphosphate. A study of *E. coli* RuvB point mutants further extends the proposition that ATP hydrolysis causes conformational changes between subunits by indicating that Arg^{174} (corresponding to Arg^{170} of *T. maritima* RuvB) acts in *trans* across the subunit interface in the RuvB hexamer (20). The Arg^{174} residue of RuvB does not comprise the active site for ATP hydrolysis in one subunit, but Arg^{174} is near the catalytic site of the adjacent subunit in the hexamer. The Walker A motif mutant K68A and R174A mutant are both deficient in ATP hydrolysis, but they were found to complement each other when mixed together (20). Hence, Arg^{174} of RuvB appears to participate *in trans* in ATP hydrolysis.

In *E. coli* RecA protein, the residues in the [KR]×[KR] motif are Lys^{248} and Lys^{250} (13). These two residues are hypothesized to be important for ATP hydrolysis and potentially communicate ATP hydrolysis between adjacent subunits in the RecA nucleoprotein filament according to the similarities to homologous proteins described above. Furthermore, the promising importance of one or both of the Lys^{248} and Lys^{250} residues was reinforced upon examination of the structure of the RecA-dsDNA nucleoprotein filament (21).

An impediment to the study of the RecA protein has been the lack of a crystal structure of the RecA filament bound to DNA. The crystal structure of the RecA filament with ADP bound (22) and the crystal structure of the RecA filament (23) provided much insight. However, RecA is a DNA-dependent ATPase, and the apo-crystal represents the inactive form of the RecA filament (21). Recently a reconstruction of the RecA filament with dsDNA, based on complexes viewed by electron microscopy, was resolved (21). The crystal structure of the RecA filament was fit within electron microscopic images of the RecA-dsDNA filament. To fit the crystal structure electron density into the electron microscopy images of the nucleoprotein filament, the RecA core was rotated and resulted in several significant structural changes. One difference between the apo-crystal structure and the electron microscopic reconstruction of the RecA-dsDNA nucleoprotein filament is location of the ATP binding site (Fig. 1). The nucleotide is bound away from the subunit-subunit interface within the filament in the apo-crystal structure. In contrast, the nucleotide is bound in between adjacent subunits in the RecA-dsDNA nucleoprotein filament reconstruction. The location of the nucleotide between two RecA subunits is supported by recent crystal structures of the archaeal RadA filament (24) and the eukaryotic Rad51 filament (25). VanLoock *et al.* (21) states there are several residues that do not contact the nucleotide in the apo-crystal structure but are near the nucleotide of the adjacent subunit in the electron microscopic reconstruction. The shifted residues include Lys^{216}, Phe^{217}, Arg^{222}, Lys^{248}, Lys^{250}, and Pro^{254}. The two residues Lys^{248} and Lys^{250} are of particular interest because, as noted above, they are the two residues that comprise the [KR]×[KR] motif in the *E. coli* RecA protein.

In this study, we sought to examine the K248 residue as an introduction to studying potential roles for the [KR]×[KR] motif in *E. coli* RecA. The K248A mutation (26) has been previously examined, and although the K248A mutant protein appears to fold normally, the K248A mutant does not form a filament. As such, we chose to introduce a more subtle mutation: K248R. We find that the K248R mutant does bind DNA and forms a nucleoprotein filament, although it hydrolyzes neither ATP nor dATP at a readily measured rate. However, we discovered that a combination of the K248R mutant and another ATP hydrolysis-deficient mutant (27, 28), E96D, partially restores dATP hydrolysis. In the nucleoprotein filament, the Lys^{248} and Glu^{96} residues are located at the subunit-subunit interface near the bound nucleotide but are opposed across the interface. Direct or indirect coordination between these two residues could be a means of communicating ATP hydrolysis-mediated conformational changes between adjacent subunits in the RecA nucleoprotein filament.

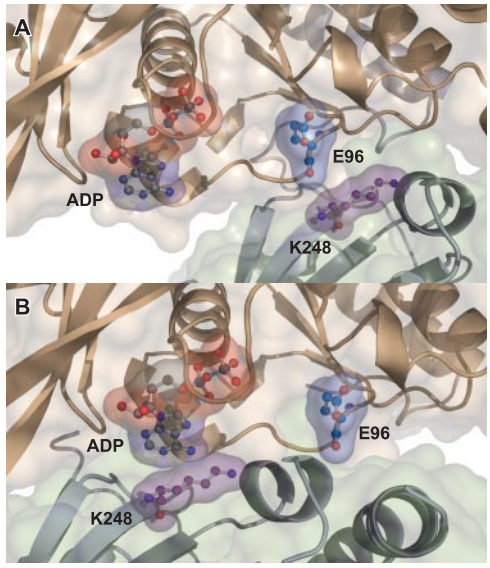

FIGURE 1. **ADP is bound in between adjacent RecA subunits in the active nucleoprotein filament.** *A*, the Glu^{96} and Lys^{248} residues of RecA are at the subunit-subunit interface of the RecA filament, as it is composed in the published three-dimensional structures (Protein Data Bank entries 1REA (22) and 2REB (23)). ADP is bound away from this interface. The apo-crystal structure of the RecA filament likely represents the inactive form of the RecA filament. *B*, an electron microscopy reconstruction of the RecA filament with dsDNA (Protein Data Bank entry 1N03 (21)) likely represents the active form of the filament and is supported by recent structures of the homologues Rad51 (35) and RadA (24). In this model, ADP is bound between adjacent subunits. Glu^{96} and Lys^{248} are both near the ADP molecule, with Lys^{248} potentially contributing to the ATP active site in *trans*.

EXPERIMENTAL PROCEDURES

Enzymes and Biochemicals—The *E. coli* SSB protein was purified as described previously (7). The *E. coli* wild type RecA protein was purified as described previously (29). The RecA K248R mutant protein was purified in the same manner as wild type. The RecA K248R/E96D double mutant protein was purified in the same manner as wild type with the following changes: the protein was eluted twice from the ammonium sulfate pellet in a solution of R Buffer (20 mM Tris-Cl buffer (80% cation, pH 7.5), 10% glycerol (w/v), 1 mM dithiothreitol) plus 150 mM ammonium sulfate. The K248R/E96D mutant protein was eluted from the DEAE-Sepharose column with a linear gradient from R Buffer plus 100 mM KCl to R Buffer plus 500 mM KCl. The K248R/E96D mutant protein was eluted from the hydroxyapatite column with a linear gradient from 20 mM phosphate buffer (10 mM KH_2PO_4, 10 mM K_2HPO_4, 10% glycerol (w/v), 1 mM dithiothreitol) to 500 mM phosphate buffer (250 mM KH_2PO_4, 250 mM K_2HPO_4, 10% glycerol (w/v), 1 mM dithiothreitol). Peak fractions were identified by SDS-PAGE, pooled and dialyzed against R Buffer, and then loaded onto a PBE-94 column (Amersham Biosciences). The K248R/E96D mutant protein was eluted with a linear

gradient from R Buffer to R Buffer plus 1 M KCl. The peak and nuclease-free fractions were pooled and concentrated with an Amicon Centricon concentrator (Millipore, Billerica, MA). The K248R/E96D mutant protein was dialyzed against R Buffer and flash-frozen in liquid nitrogen and finally stored at −80 °C. The E96D mutant RecA protein was purified similarly to the K248R/E96D mutant, excluding the PBE-94 column.

The purified RecA protein (both mutants and wild type) and SSB protein concentrations were determined by absorbance at 280 nm, using extinction coefficients of $\epsilon_{280} = 2.23 \times 10^4\ \text{M}^{-1}\ \text{cm}^{-1}$ (30) and $\epsilon_{280} = 2.38 \times 10^4\ \text{M}^{-1}\ \text{cm}^{-1}$ (31), respectively. RecA protein and SSB preparations were free of detectable endo- and exonuclease activities on dsDNA and ssDNA. Unless otherwise noted, all reagents were purchased from Fisher. Phosphoenolpyruvate (PEP), pyruvate kinase, lactate dehydrogenase, phosphocreatine, ATP, dATP, and NADH were purchased from Sigma. Creatine kinase and ATPγS were purchased from Roche Applied Science. Restriction enzymes were purchased from New England Biolabs (Beverly, MA). Dithiothreitol was purchased from Research Organics (Cleveland, OH).

DNA Substrates—Poly(dT) was purchased from Amersham Biosciences, and the approximate average length is 229 nucleotides. Bacteriophage ΦX174 circular ssDNA and replicative form I supercoiled circular duplex DNA were purchased from New England Biolabs and Invitrogen, respectively. Full-length linear duplex DNA (dsDNA) was generated by digesting ΦX174 replicative form I DNA (5386 bp) with the XhoI endonuclease. Circular single-stranded DNA from bacteriophage M13mp8 (7229 nucleotides) was prepared as described (32). Concentrations of ssDNA and dsDNA were determined by absorbance using 108 and 151 μM A_{260}^{-1}, respectively, as conversion factors. All DNA concentrations are given in micromolar nucleotide concentrations.

Circular Dichroism—Wild type RecA protein and two separate preparations of the RecA K248R/E96D double mutant protein were analyzed on a model Aviv 62A DS circular dichroism Spectrometer (Aviv, Lakewood, NJ) equipped with a temperature controller. For each protein, the solution included 0.25 mg/ml protein, 10 mM KH_2PO_4, and 10 mM K_2HPO_4. The solutions were measured at 4 °C and 37 °C. Graphs of wavelength (nm) *versus* molar ellipticity (degree $\text{cm}^2\ \text{dmol}^{-1} \times 10^{-4}$) were normalized with respect to the absolute minimum at 208 nm. The RecA K248R/E96D protein CD spectrum and wild type RecA protein CD spectrum were superimposed to identify any differing points on the graphs. Two separate preparations of the RecA K248R/E96D mutant protein were examined.

Reaction Conditions—All reactions were carried out at 37 °C in 25 mM Tris acetate buffer (80% cation, pH 7.5), 10 mM magnesium acetate, 5% (v/v) glycerol, 1 mM dithiothreitol, 3 mM potassium glutamate, 3 mM ATP or dATP, an ATP regenerating system (10 units/ml pyruvate kinase and 3 mM PEP), and concentrations of DNA and RecA protein were as described below and in the figure legends to Figs. 2 and 4–7. The coupled spectrophotometric assay also contained 10 units/ml lactate dehydrogenase and 1.5 or 0.15 mM NADH. DNA and protein concentrations are indicated for each experiment. Reactions were incubated for 10 min before ATP or dATP was added to start the reaction.

ATP Hydrolysis Assays—A coupled spectrophotometric assay (33, 34) was used to measure ATP and dATP hydrolysis by the RecA protein (29). The regeneration of ATP or dATP from ADP and PEP was coupled to the oxidation of NADH and monitored by the decrease in absorbance of NADH at 380 or 340 nm. The 380-nm wavelength was used instead of the absorption maximum at 340 nm so that the signal would remain within the linear range of the spectrophotometer for the duration of the experiment. However, the 340-nm wavelength was used instead of 380 nm to increase the sensitivity of the assay when the hydrolysis rate was slow. The assay was carried out using a Varian Cary 300 (Varian, Palo Alto, CA) dual beam spectrophotometer equipped with a temperature controller and 12-position cell changer. The cell path length and band pass were 1.0 cm and 2 nm, respectively. The NADH extinction coefficients at 380 nm of 1.21 $\text{mM}^{-1}\ \text{cm}^{-1}$ and at 340 nm of 6.22 $\text{mM}^{-1}\ \text{cm}^{-1}$ were used to calculate rates of ATP or dATP hydrolysis.

DNA Three-strand Exchange Reactions—DNA three-strand exchange reactions were carried out at 37 °C in 25 mM Tris acetate buffer (80% cation, pH 7.5). RecA protein (up to 3 μM) was preincubated with ΦX174 circular ssDNA (up to 10 μM) for 10 min. SSB protein (to 1 μM) and dATP (to 3 mM) were then added, followed by another 10-min incubation. The reactions were initiated by the addition of ΦX174 linear dsDNA to 10 μM. Reactions were incubated for a total of 120 min with a 10-μl sample taken at 0, 15, 30, 45, 60, 90, and 120 min. Reactions were stopped and analyzed by gel electrophoresis as described (35).

Electron Microscopy—A modified Alcian method was used to visualize RecA filaments. Activated grids were prepared as described previously (29). Reaction mixtures included 25 mM Tris acetate buffer (80% cation, pH 7.5), 10 mM magnesium acetate, 5% (v/v) glycerol, 3 mM potassium glutamate, an ATP regenerating system (12 mM phosphocreatine and 10 units/ml creatine kinase), 6 μM poly(dT) linear ssDNA, and 8 μM total RecA. Reactions were incubated at 37 °C for 10 min before dATP (to 3 mM) was added to start the filament formation. The reaction was again incubated at 37 °C for 10 min to allow RecA to form a filament on the DNA. ATPγS was then added to 3 mM, and the reaction was incubated at 37 °C for 3 min to stabilize the RecA-DNA filament. The reaction solution was then diluted 5- or 10-fold in buffer (200 mM ammonium acetate, 10 mM HEPES, pH 7.5, and 10% glycerol) and prepared for spreading onto grids. Digital images of the nucleoprotein filaments were taken at ×15,000 magnification. Filament lengths were measured using MetaMorph analysis software (Molecular Devices). At least 50 filaments were measured for each RecA protein. Each filament was measured three times, and the average length was calculated. Filaments less than 30 nm long were difficult to distinguish from the background and were not included in the analysis.

A cytochrome *c* method was used to visualize poly(dT) linear ssDNA as a control. Samples were prepared as described previously (36), except the spreading solution was assembled by combining 32 μl of 1 M Na_2CO_3, 40 μl of 0.126 M Na_2EDTA, 400 μl of 37% HCHO, 292 μl of 100% formamide, and 10 μl of 5 M KOH. The final DNA concentration was 0.004 μg/μl.

RESULTS

Experimental Design—We focused on the contribution of two residues at the subunit-subunit interface of the nucleoprotein filament to catalysis of ATP hydrolysis by the RecA protein. Using purified proteins, we examined the ATP hydrolysis activity of the K248R and E96D single mutants and the K248R/E96D double mutant RecA proteins. Mixtures of the K248R and E96D single mutant proteins were also examined. RecA-mediated ATP hydrolysis is DNA-dependent. Electron microscopy was used to help determine to what extent the observed rates of ATP hydrolysis, when reduced in the case of a mutant RecA protein, result directly from a catalytic impairment or indirectly from an inability to bind DNA and form nucleoprotein filaments. The effect of the reduced ATP hydrolysis rate on the ability of the mutants to catalyze the *in vitro* DNA three-strand exchange reaction was also examined. This allows us to uncover the contribution of nucleoprotein filament formation to the catalysis of ATP hydrolysis by the RecA protein and a poten-

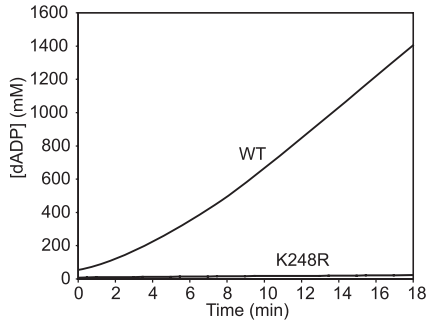

FIGURE 2. **The K248R RecA protein does not hydrolyze dATP DNA-dependently relative to wild type.** RecA-catalyzed dATP hydrolysis was monitored. The top curve represents hydrolysis for wild type RecA protein, and the lower curve represents hydrolysis for the K248R mutant RecA protein. Reactions included 8 μM RecA protein and 6 μM poly(dT) linear ssDNA. The RecA protein was preincubated with the DNA for 10 min before dATP was added. Time 0 corresponds to the time of dATP addition. The average observed rates of dATP hydrolysis were 92.45 $\pm$ 1.91 and 0.57 $\pm$ 0.14 μM/min for wild type and K248R RecA protein, respectively.

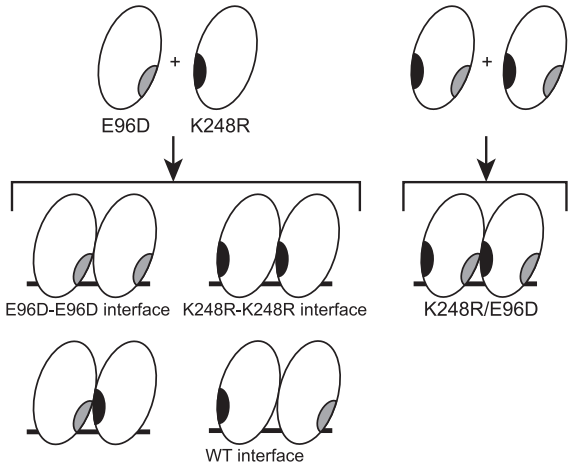

FIGURE 3. **A mixture of the K248R and E96D single RecA mutants would result in a nucleoprotein filament with a mixture of four possible subunit-subunit interfaces.** The mixture of K248R and E96D mutant protomers could form four different subunit-subunit interfaces to assemble a nucleoprotein filament. Two K248R subunits could be adjacent in the filament to form the K248R-K248R interface. Two E96D subunits could be adjacent in the filament to mimic the E96D-E96D interface. The K248R and E96D subunits could be adjacent in the filament in two possible orientations: one would mimic the wild type RecA subunit-subunit interface, while the other would combine both the K248R and E96D mutations at the subunit-subunit interface. This last interface would mimic the subunit-subunit interface formed by the K248R/E96D double mutant RecA protein, depicted on the *right*.

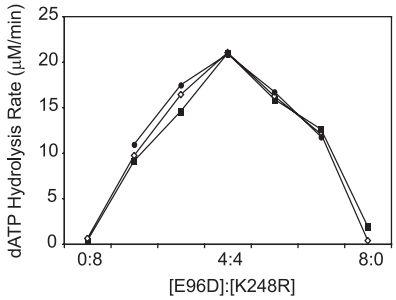

FIGURE 4. **A mixture of the K248R and E96D single mutant RecA proteins on poly(dT) hydrolyzes optimally at a ratio of 1 K248R:1 E96D.** RecA-catalyzed dATP hydrolysis was monitored. Reactions included 8 μM total RecA protein, 6 μM poly(dT) linear ssDNA, and dATP. The assay was done in triplicate (all assays are shown). The optimal rate of dATP hydrolysis was observed at a 1:1 ratio of the two single mutants. This rate of dATP hydrolysis, 20.91 $\pm$ 0.08 μM/min, was ~23% of the rate seen with wild type RecA protein alone under the same reaction conditions (91.54 $\pm$ 2.86 μM/min).

tial means of molecular communication between adjacent RecA subunits.

The K248R RecA Mutant Does Not Hydrolyze ATP—The K248R mutant hydrolyzed ATP or dATP at a minimal rate relative to the wild type *E. coli* RecA protein (Fig. 2). The elimination of ATP and dATP hydrolysis indicated that the Lys^{248} residue is critical for catalysis. As described below, the K248R mutant was still able to form short nucleoprotein filaments on DNA, indicating that the mutation does not perturb the subunit-subunit interface enough to completely prevent filament formation. From these initial observations, it was not clear whether the Lys^{248} residue might act in *cis* or in *trans* to promote hydrolysis. A RecA nucleoprotein filament reconstruction suggests Lys^{248} acts in *trans* across the subunit-subunit interface.

A Combination of the E96D and K248R Mutations Partially Restores ATP Hydrolysis Activity—In an effort to partially restore ATP hydrolysis activity to the K248R filament, the K248R protein was mixed with the E96D mutant in different ratios. In such mixtures of the two single mutants, the resulting mixed filament would have four possible subunit-subunit interfaces, depicted in Fig. 3. Two adjacent K248R subunits would create an interface that mimics all interfaces of the K248R filament. Two adjacent E96D subunits would create a second interface, mimicking all interfaces of the E96D filament. Adjacent E96D and K248R subunits could align in two possible orientations: one mimics the E96D/K248R double mutant and the other mimics the wild type interface. We hypothesized that the wild type interface formed by the mixture of the E96D and K248R single mutants would hydrolyze dATP, thus partially rescuing catalysis of ATP hydrolysis. The E96D and K248R single mutants were mixed in varying ratios from 3:1 to 2:1 to 1:1. As shown in Fig. 4, the greatest rate of hydrolysis was observed for the 1:1 ratio of the E96D and K248R single mutants. The 1:1 mixture of the two single mutants restored dATP hydrolysis to 25% of the wild type rate.

The observed hydrolysis rate of the E96D and K248R mixed filament led to the following model. When mixed at a ratio of 1:1, the four possible interfaces (Fig. 3) would have an equal probability of forming. It was initially thought that only one of the four possible interfaces would hydrolyze dATP. That is, the E96D:E96D interface would not hydrolyze, the K248R:K248R interface would not hydrolyze, the K248R:E96D interface would not hydrolyze, but the interface mimicking the wild type interface *would* hydrolyze at 100% of the wild type rate. According to this model, the rate of hydrolysis for the 1:1 mixture of E96D and K248R would be 25% of the wild type rate as was observed.

To test the model, the K248R/E96D double mutant was examined. As shown in Fig. 5, the double mutant did hydrolyze dATP, although still at a reduced rate compared with the wild type rate. The K248R and E96D mutants did not individually hydrolyze dATP, but together, the two point mutations restored partial hydrolysis activity.

The Mutant RecA Proteins Form Nucleoprotein Filaments—To confirm that the reduced rate of hydrolysis was not indirectly due to misfolding of the protein, circular dichroism spectra of the K248R/E96D double mutant were compared with that of the wild type RecA protein. Spectra of the mutant and wild type RecA proteins were identical, indicating the K248R/E96D protein folded as well as wild type. Two different preparations of the K248R/E96D mutant yielded the same results (data not shown).

The DNA-independent rate of hydrolysis was examined. Wild type RecA, E96D, K248R, K248R/E96D, and the E96D+K248R mixture did not readily hydrolyze ATP or dATP in the absence of DNA (Fig. 5), indicating the observed nucleotide hydrolysis for wild type, K248R/E96D, and the E96D+K248R protein mixture was dependent on the presence of DNA.

We used electron microscopy to visualize wild type and mutant RecA proteins bound to DNA. As shown in Fig. 6, wild type RecA and the mutants formed filaments on poly(dT) at pH 7.5 with dATP. No fila-

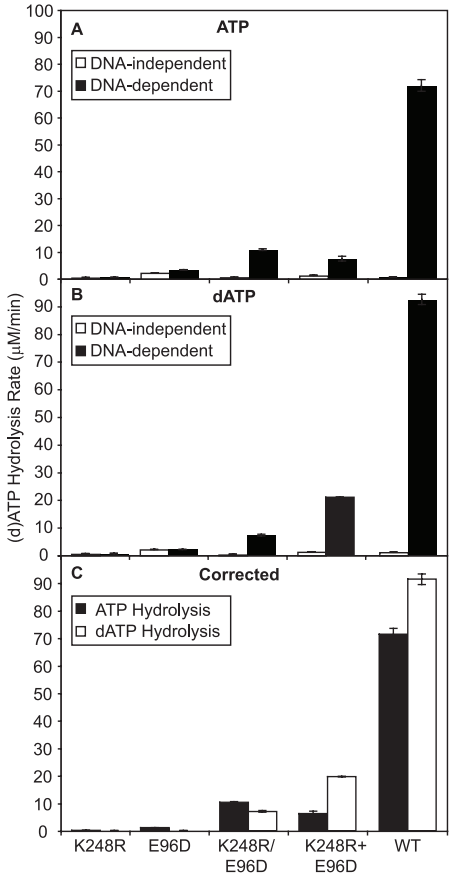

FIGURE 5. **The mixture of K248R+E96D mutants and the K248R/E96D double mutant RecA protein partially restores DNA-dependent ATP and dATP hydrolysis.** RecA-catalyzed dATP or ATP hydrolysis was monitored. Reactions included 8 μM RecA protein, 6 μM poly(dT) linear ssDNA (when included), and dATP or ATP. The rates of hydrolysis were calculated for several trials with and without poly(dT) linear ssDNA for both ATP (*A*) and dATP (*B*) substrates. The average for each data set is plotted for each RecA protein. *C*, for each ATP or dATP data set, the rates of DNA-independent hydrolysis were averaged. The average rate of DNA-independent hydrolysis was then subtracted from each DNA-dependent rate of hydrolysis to result in the corrected rate of hydrolysis. The corrected rates of hydrolysis were then averaged and plotted for each RecA protein. Both E96D and K248R hydrolyzed neither ATP nor dATP at significant rates relative to wild type RecA protein. The 1:1 mixture of the K248R and E96D proteins hydrolyzed both ATP and dATP and hydrolyzed dATP at ~25% of the wild type dATP hydrolysis rate. The K248R/E96D double mutant RecA protein also hydrolyzed both ATP and dATP, and the double mutant restored dATP hydrolysis to ~8% of the wild type dATP hydrolysis rate.

ments were seen without the presence of DNA (data not shown), implying that the filaments were DNA-dependent. Both wild type and E96D RecA proteins formed filaments from 30 to over 1000 nm in length with most filaments over 600 nm. K248R and K248R/E96D RecA proteins formed shorter filaments. The E96D+K248R mixed filaments were a range of lengths, mostly 500–600 nm in length.

The poly(dT) linear ssDNA is present in a range of lengths, with an average of 229 nucleotides. This length is quite short (encompassing no more than ~120 nm when bound by RecA protein), and the poly(dT) was not seen by itself in electron micrographs at ×15,000 magnification (data not shown). The longer RecA nucleoprotein filaments reflect multiple RecA-poly(dT) complexes that RecA has joined together noncovalently end-to-end via interactions between the terminal RecA subunits in adjacent complexes. The filaments including the K248R mutation were much shorter, suggesting that this mutation somewhat impairs the joining of filament ends.

The Partial Restoration of ATP Hydrolysis Is Insufficient to Catalyze DNA Three-strand Exchange—Wild type RecA catalyzes an efficient three DNA strand exchange reaction, forming nicked circular product within 30–45 min. No nicked circular product formation was observed for E96D, K248R, K248R/E96D, or the 1:1 mixture of E96D and K248R single mutants with ΦX174 DNA (data not shown). The partial restoration of catalysis of ATP and dATP hydrolysis by K248R/E96D and the 1:1 mixture of E96D and K248R were insufficient to promote complete strand exchange. It was previously known that nucleotide hydrolysis is required for DNA strand exchange for long DNA substrates (longer than 3 kbp), DNA strand exchange with four DNA strands, and strand exchange past barriers in the DNA such as an insertion of multiple DNA base pairs in one of the DNA substrates (4–8). Hence, the results support the notion that ATP hydrolysis must occur throughout the filament to complete nicked circular product formation with ΦX174 DNA molecules.

K248R/E96D Nucleoprotein Filament Is Unable to Displace SSB during Filament Extension—Nucleation of wild type RecA onto ssDNA is inhibited by SSB prebound to the DNA. Once RecA has nucleated onto the DNA, however, addition of SSB to the reaction stimulates extension of the RecA filament. SSB binds to and melts secondary structure in the DNA, thus enabling extension of the RecA filament. All experiments described above were completed with poly(dT) linear ssDNA that has a reduced propensity to form secondary structure, thus eliminating the need for SSB. With M13mp8 circular ssDNA, however, secondary structure in the DNA can form and adding SSB to the reaction after nucleation of wild type RecA then stimulates complete formation of the nucleoprotein filament and maximal ATP or dATP hydrolysis. In contrast, the K248R/E96D double mutant did not hydrolyze ATP or dATP with M13mp8 when SSB was added after a time sufficient to permit RecA nucleation, indicating a complete K248R/E96D filament did not form in the presence of SSB.

To examine the effect of SSB further, the dATP hydrolysis of wild type RecA and K248R/E96D were compared on M13mp8 with and without SSB. Reactions included RecA protein and M13mp8 circular ssDNA and were initiated by the addition of dATP. As shown in Fig. 7, both wild type RecA and K248R/E96D hydrolyzed dATP at a substantial but reduced rate compared with the maximal rate observed on poly(dT). Both wild type RecA and K248R/E96D were able to form significant nucleoprotein filaments on M13mp8 circular ssDNA in the absence of SSB. SSB was then added to the reactions after ~20 min. As shown in Fig. 7, wild type RecA hydrolyzed dATP at the maximal rate almost immediately upon addition of SSB to the reaction, indicating that SSB facilitated the extension of a complete nucleoprotein filament on M13mp8. Conversely, dATP hydrolysis catalyzed by K248R/E96D was reduced and progressively eliminated upon addition of SSB to the reaction, suggesting that K248R/E96D was unable to displace SSB from the DNA during extension of the nucleoprotein filament (and in fact the SSB was replacing the RecA mutant protein). These combined two mutations at the subunit-subunit interface of RecA appeared to only disturb filament formation when RecA protein is presented with a barrier, such as SSB prebound to the DNA. The binding affinity of RecA protein needed to compete with SSB has thus been reduced by the mutation, possibly as a result of a decrease in the contribution of subunit-subunit cooperativity to overall RecA filament stability.

DISCUSSION

We conclude that K248R and E96D positively cooperate across the subunit-subunit interface of RecA to catalyze ATP hydrolysis, thus implying the catalytic participation of Lys^{248} in ATP hydrolysis of the adjacent subunit in the RecA nucleoprotein filament. These two residues appear to be closely opposed across the subunit-subunit interface in an active RecA filament. The effects of complementing one mutation

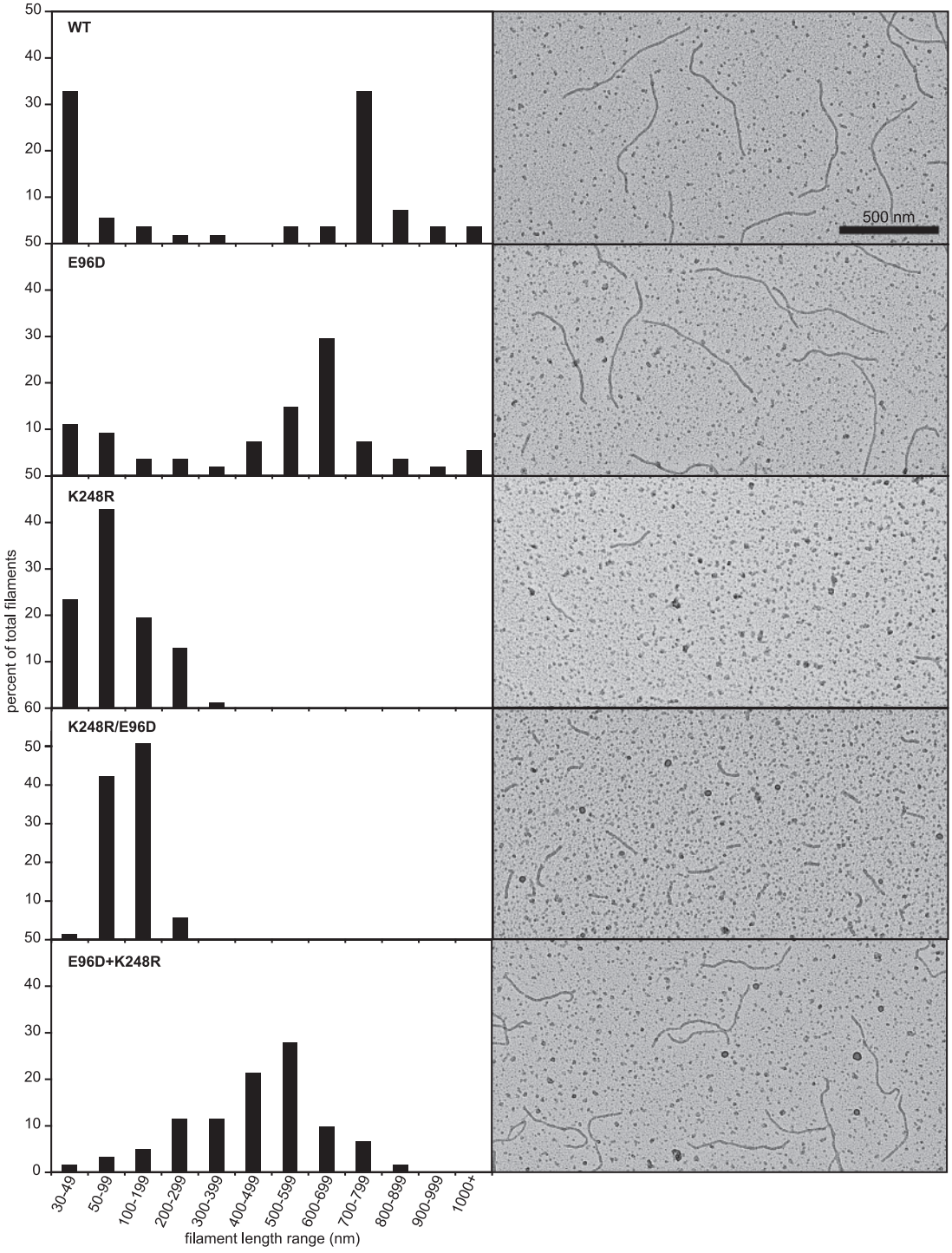

FIGURE 6. **Wild type (WT) RecA and mutants form DNA-dependent nucleoprotein filaments.** Electron micrographs show wild type and mutant RecA filaments on linear ssDNA. Reactions included 8 μM RecA protein and 6 μM poly(dT) linear ssDNA. The RecA protein was preincubated with the DNA for 10 min before dATP was added. The reaction was incubated for 10 min more to permit filament formation. Then ATPγS was added (to 3 mM) and the reaction incubated for 3 min to stabilize the filaments. Reactions were diluted 10-fold, except the K248R reaction (5-fold), before adhesion to the electron microscopy (alcians) grid. Nucleoprotein filaments were viewed with the electron microscope. For each protein, a total of at least 50 representative filaments were measured. Filaments shorter than 30 nm were difficult to distinguish from background and were not included in the reported totals. The results may thus underestimate the representation of shorter filament forms, especially for the K248R mutant. A histogram of filament length is shown for each protein next to the electron microscopy image. Wild type and E96D RecA proteins formed a range of nucleoprotein filament lengths with many long filaments greater than 600 nm. Since this is far longer than the available lengths of poly(dT), this implies an end-to-end joining of nucleoprotein filaments. The K248R and K248R/E96D mutant proteins only formed filaments with shorter lengths. The K248R filaments of measurable length were also present at a much reduced concentration. The E96D+K248R mixed filaments were a range of lengths, mostly median to the wild type and K248R filament lengths. All filaments are DNA-dependent, as no filaments were seen in the absence of DNA (data not shown).

with the other could be direct or indirect. However, the results suggest an in *trans* participation of Lys^{248} and perhaps other residues in the ATP hydrolytic cycle. The cross-interface connection may help to organize ATP hydrolytic cycle-induced conformational changes between adjacent subunits.

Lys^{248} of *E. coli* RecA is conserved among bacterial RecA homologues

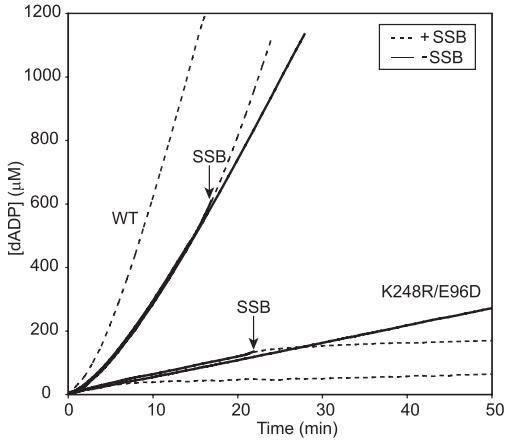

FIGURE 7. **The extending K248R/E96D mutant RecA protein filament is compromised and does not displace SSB.** RecA-catalyzed dATP hydrolysis was monitored. Reactions included 8 μM RecA protein, 6 μM M13mp8 circular ssDNA, 0.6 μM SSB (when included), and dATP. The RecA protein was preincubated with the DNA for 10 min before dATP was added to initiate the reaction. Time 0 corresponds to the time of dATP addition. For both RecA proteins, there are three conditions: SSB was added initially with dATP (*contiguous dashed line*), SSB was added ~20 min after dATP addition (*solid line* continued as *dashed* after SSB addition indicated by an *arrow*), or SSB storage buffer was added ~20 min after dATP addition (*continuous solid line*). The *top three curves* represent hydrolysis by the wild type RecA protein; the *bottom three curves* represent hydrolysis by the K248R/E96D RecA protein. The *solid curves* represent dATP hydrolysis before SSB protein was added to the reaction; the *dashed lines* represent dATP hydrolysis after the addition of SSB protein.

(13). Some structural studies indicate that Lys^{248} is too distant to contribute to an ATP hydrolysis catalytic site within a RecA protomer (22, 23). However, a more recent electron microscopic reconstruction of the RecA-dsDNA nucleoprotein filament (21), coupled to the overall subunit-subunit interface seen in recently determined structures of the RecA homologues Rad51 (25) and RadA (24), suggests that Lys^{248}, along with several other residues, lies in proximity to the nucleotide binding site of the adjacent subunit. Hence, Lys^{248} may contribute to nucleotide hydrolysis in the neighboring subunit in *trans*. Further support of this notion is the discovery of the [KR]×[KR] motif in RecA and helicases including T7 gp4 that is postulated to be involved in in *trans* catalysis of ATP hydrolysis and communication of the ATP hydrolytic cycle between subunits or domains (13–16, 18–20). Lys^{248} is the first residue in the [KR]×[KR] motif of *E. coli* RecA (13). The effects of a conservative mutation introduced at residue 248, K248R, indicate Lys^{248} is crucial for ATP hydrolysis but at least partly dispensable for DNA binding and filament formation. The Glu^{96} residue is part of the ATP binding site within a single RecA subunit, and the E96D mutant also does not readily hydrolyze ATP. A mixture of K248R and E96D restored ATP hydrolysis activity to the nucleoprotein filament. Complementation of E96D and K248R together with the location of these residues at the subunit-subunit interface in the nucleoprotein filament illustrates the importance of this interface to nucleotide hydrolysis and suggests an in *trans* catalysis mechanism of nucleotide hydrolysis whereby the adjacent RecA subunit contributes catalytically.

Both the K248R and E96D single mutants of RecA protein will bind to ssDNA and form filaments. The K248R mutant has a reduced capacity to tandemly and noncovalently link short filaments to create longer ones, indicating a somewhat compromised subunit-subunit interface. Nevertheless, the capacity of both mutant proteins to bind to poly(dT) suggests that their inability to hydrolyze ATP or dATP is primarily due to a catalytic defect in ATP hydrolysis and not indirectly from an inability to form a filament on DNA. Despite K248R and E96D both being deficient in ATP and dATP hydrolysis activity, partial dATP hydrolysis activity is restored (to 25% of the wild type RecA hydrolysis rate) when these two mutants are mixed at a 1:1 ratio. Perhaps more surprisingly, the K248R/E96D double mutant protein promotes dATP hydrolysis at a rate that is more than 10-fold greater than either of the single mutants alone when bound to poly(dT). The restored hydrolysis is due at least in part to the formation of some wild type subunit-subunit interfaces that hydrolyze dATP or ATP when the K248R and E96D single mutants are mixed. However, the observation that the K248R/E96D double mutant hydrolyzes ATP and dATP indicates that the subunit-subunit interface formed when the K248R and E96D mutations are opposed to each other across the interface is also at least partially enabled for hydrolysis. The Glu^{96} residue may activate the water molecule for nucleophilic attack in ATP hydrolysis (22). An aspartate at this location would necessarily affect this reaction. The presence of an arginine at position 248 may perturb the structure at the interface to bring the γ-phosphate of the ATP molecule and the mutant aspartate residue at position 96 in closer proximity to the nucleophilic water molecule. Conceivably the K248R mutation, when present with the normal Glu^{96} across the interface, could destabilize the interface and prevent ATP hydrolysis. We do not know if the distribution of the two single mutant proteins in the mixed filament is random but would argue that it is unlikely that the distribution of mutant proteins would leave the wild type subunit-subunit interfaces underrepresented. If 25% of the interfaces formed mimic the wild type interface to hydrolyze dATP (Fig. 3), and 25% of interfaces mimic the K248R/E96D interface to hydrolyze dATP as well, then the wild type interfaces in the mixed filaments must be hydrolyzing dATP at less than 100% of the wild type efficiency to arrive at the observed rates. The results thus suggest that longer range coordination of ATP hydrolytic cycles occurs in the filaments; adjacent subunit-subunit interfaces affect each other. This conclusion suggests the importance of contiguous hydrolysis-enabled interfaces in the RecA nucleoprotein filament.

An extending K248R/E96D filament on ssDNA does not displace SSB, whereas wild type RecA is able to displace SSB and extend a filament. The K248R mutation must introduce instability at the subunit-subunit interface, despite the cooperation with E96D. The less robust interaction at the subunit-subunit interface impedes filament formation against a barrier, such as SSB.

These results indicate that each of the two single mutants, K248R and E96D, has a distinct catalytic defect and partial restoration of nucleotide hydrolysis results from a complementary interaction of the K248R and E96D residues between adjacent subunits in *trans*. The results suggest that the Lys^{248} residue has an intermolecular catalytic role in nucleotide hydrolysis in the RecA nucleoprotein filament. Coordination of ATP hydrolysis between adjacent subunits as observed recently (9) may manifest through Lys^{248}. The Lys^{248} residue of *E. coli* RecA presents another example of the [KR]×[KR] motif acting across a subunit or domain interface to catalyze ATP hydrolysis and potentially direct conformational changes dependent on the nucleotide state. This is a developing mechanism for motor ATPase proteins with RecA-like protein folds.

The lack of a [KR]×[KR] motif in the archaeal and eukaryotic members of the RecA family is intriguing. RecA promotes a number of DNA transactions, all requiring ATP hydrolysis, which the RadA, Rad51, and Dmc1 proteins are not able to promote. The [KR]×[KR] motif may provide an important clue to help understand the molecular basis of this distinction.

Acknowledgments—We thank Elizabeth A. Wood for cloning of the RecA mutant proteins. We also thank the Clagett-Dame Laboratory at the University of Wisconsin-Madison Department of Biochemistry for use of their MetaMorph analysis software. Finally, we are very grateful to Dr. Edward Egelman (University of Virginia) for reading and commenting on this manuscript.

REFERENCES

1. Lusetti, S. L., and Cox, M. M. (2002) *Annu. Rev. Biochem.* **71,** 71–100
2. Cox, M. M., Goodman, M. F., Kreuzer, K. N., Sherratt, D. J., Sandler, S. J., and Marians, K. J. (2000) *Nature* **404,** 37–41
3. Schlacher, K., Leslie, K., Wyman, C., Woodgate, R., Cox, M. M., and Goodman, M. F. (2005) *Mol. Cell* **17,** 561–572
4. Jain, S. K., Cox, M. M., and Inman, R. B. (1994) *J. Biol. Chem.* **269,** 20653–20661
5. Kim, J. I., Cox, M. M., and Inman, R. B. (1992) *J. Biol. Chem.* **267,** 16444–16449
6. Kim, J. I., Cox, M. M., and Inman, R. B. (1992) *J. Biol. Chem.* **267,** 16438–16443
7. Shan, Q., Cox, M. M., and Inman, R. B. (1996) *J. Biol. Chem.* **271,** 5712–5724
8. Cox, M. M. (2003) *Annu. Rev. Microbiol.* **57,** 551–577
9. Cox, J. M., Tsodikov, O. V., and Cox, M. M. (2005) *PLoS Biol.* **3,** 231–243
10. Robu, M. E., Inman, R. B., and Cox, M. M. (2001) *Proc. Natl. Acad. Sci. U. S. A.* **98,** 8211–8218
11. Robu, M. E., Inman, R. B., and Cox, M. M. (2004) *J. Biol. Chem.* **279,** 10973–10981
12. Ye, J., Osborne, A. R., Groll, M., and Rapoport, T. A. (2004) *Biochim. Biophys. Acta* **1659,** 1–18
13. Leipe, D. D., Aravind, L., Grishin, N. V., and Koonin, E. V. (2000) *Genome Res.* **10,** 5–16
14. Sawaya, M. R., Guo, S., Tabor, S., Richardson, C. C., and Ellenberger, T. (1999) *Cell* **99,** 167–177
15. Singleton, M. R., Sawaya, M. R., Ellenberger, T., and Wigley, D. B. (2000) *Cell* **101,** 589–600
16. Crampton, D. J., Guo, S., Johnson, D. E., and Richardson, C. C. (2004) *Proc. Natl. Acad. Sci. U. S. A.* **101,** 4373–4378
17. Scheffzek, K., Lautwein, A., Kabsch, W., Reza Ahmadian, M., and Wittinghofer, A. (1996) *Nature* **384,** 591–596
18. Putnam, C. D., Clancy, S. B., Tsuruta, H., Gonzalez, S., Wetmur, J. G., and Tainer, J. A. (2001) *J. Mol. Biol.* **311,** 297–310
19. Yamada, K., Kunishima, N., Mayanagi, K., Ohnishi, T., Nishino, T., Iwasaki, H., Shinagawa, H., and Morikawa, K. (2001) *Proc. Natl. Acad. Sci. U. S. A.* **98,** 1442–1447
20. Hishida, T., Han, Y.-W., Fujimoto, S., Iwasaki, H., and Shinagawa, H. (2004) *Proc. Natl. Acad. Sci. U. S. A.* **101,** 9573–9577
21. VanLoock, M. S., Yu, X., Yang, S., Lai, A. L., Low, C., Campbell, M. J., and Egelman, E. H. (2003) *Structure (Camb.)* **11,** 1–20
22. Story, R. M., and Steitz, T. A. (1992) *Nature* **355,** 374–376
23. Story, R. M., Weber, I. T., and Steitz, T. A. (1992) *Nature* **355,** 318–325
24. Wu, Y., He, Y., Moya, I. A., Qian, X. G., and Luo, Y. (2004) *Mol. Cell* **15,** 423–435
25. Conway, A. B., Lynch, T. W., Zhang, Y., Fortin, G. S., Fung, C. W., Symington, L. S., and Rice, P. A. (2004) *Nat. Struct. Mol. Biol.* **11,** 791–796
26. Nguyen, T. T., Muench, K. A., and Bryant, F. R. (1993) *J. Biol. Chem.* **268,** 3107–3113
27. Campbell, M. J., and Davis, R. W. (1999) *J. Mol. Biol.* **286,** 417–435
28. Campbell, M. J., and Davis, R. W. (1999) *J. Mol. Biol.* **286,** 437–445
29. Lusetti, S. L., Wood, E. A., Fleming, C. D., Modica, M. J., Korth, J., Abbott, L., Dwyer, D. W., Roca, A. I., Inman, R. B., and Cox, M. M. (2003) *J. Biol. Chem.* **278,** 16372–16380
30. Craig, N. L., and Roberts, J. W. (1981) *J. Biol. Chem.* **256,** 8039–8044
31. Lohman, T. M., and Overman, L. B. (1985) *J. Biol. Chem.* **260,** 3594–3603
32. Neuendorf, S. K., and Cox, M. M. (1986) *J. Biol. Chem.* **261,** 8276–8282
33. Lindsley, J. E., and Cox, M. M. (1990) *J. Biol. Chem.* **265,** 9043–9054
34. Morrical, S. W., Lee, J., and Cox, M. M. (1986) *Biochemistry* **25,** 1482–1494
35. Drees, J. C., Lusetti, S. L., Chitteni-Pattu, S., Inman, R. B., and Cox, M. M. (2004) *Mol. Cell* **15,** 789–798
36. Schnos, M., and Inman, R. B. (2000) *Mol. Biotechnol.* **16,** 77–86